



Supplementary Information for

Direct imaging of rapid tethering of synaptic vesicles accompanying exocytosis at a fast central synapse

Takafumi Miki^{a,b,1}, Mitsuharu Midorikawa^c, and Takeshi Sakaba^{a,1}

^aGraduate School of Brain Science, Doshisha University, Kyoto 610-0394, Japan

^bOrganization for Research Initiatives and Development, Doshisha University, Kyoto 610-0394, Japan

^cDivision of Neurophysiology, Department of Physiology, School of Medicine, Tokyo Women's Medical University, Tokyo 162-8666, Japan

¹Corresponding authors: Takeshi Sakaba and Takafumi Miki

Email: tsakaba@mail.doshisha.ac.jp tmiki@mail.doshisha.ac.jp

This PDF file includes:

Figures S1 to S4

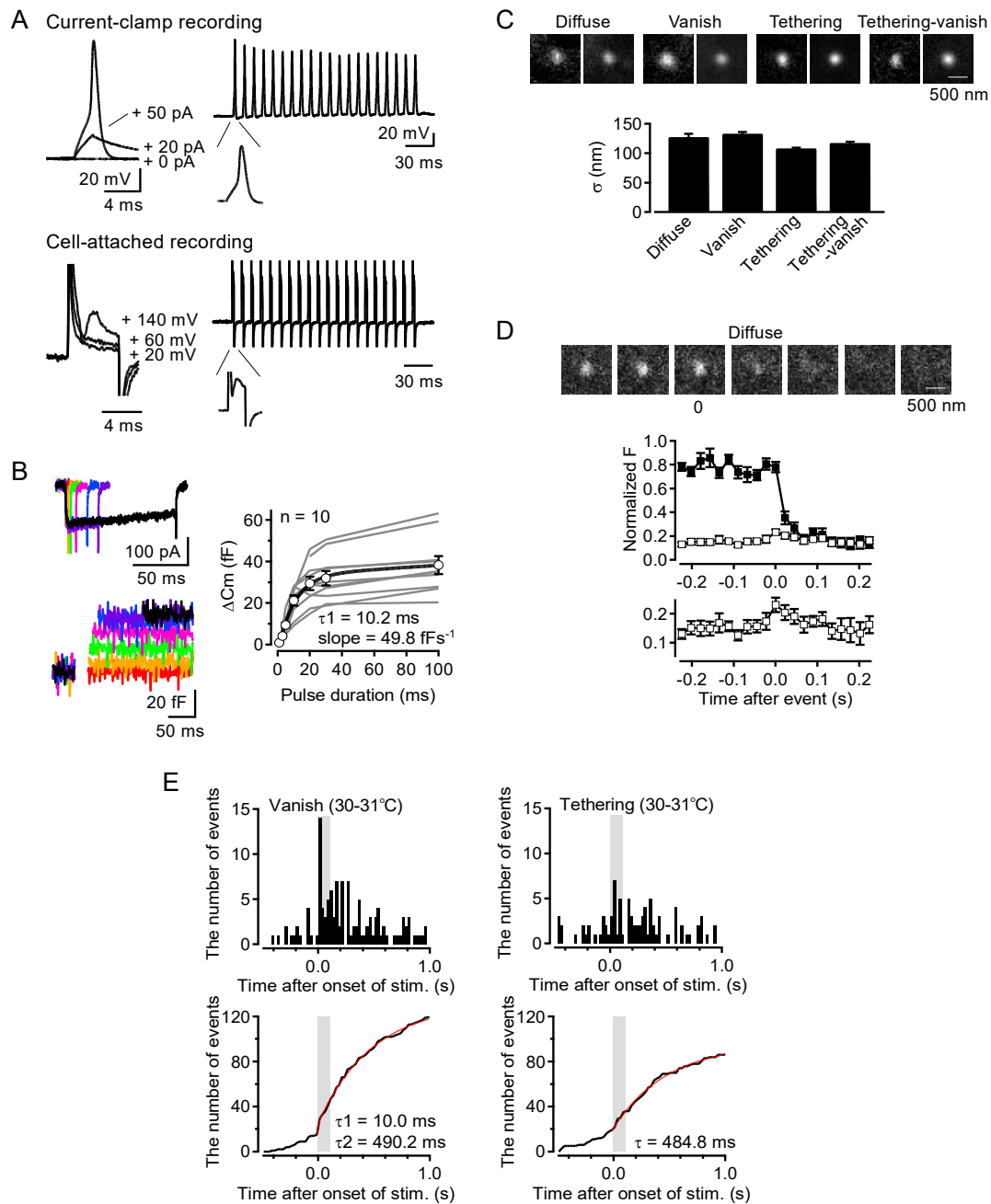


Fig. S1. Electrophysiological properties and TIRF imaging of dissociated cMF terminals.

(A) Top, example traces of current-clamp recordings from a dissociated cMF terminal. Left, 0, 25, and 50 pA current steps for 2 ms were applied. Right, 2-ms current steps were applied at 100 Hz. Bottom, example traces of cell-attached recording from a dissociated cMF terminal. Left, 20, 60, and 140 mV voltage step for 5 ms were applied. An AP-associated current was observed at 140 mV-voltage step. The negative peak during the step correspond to the time point of maximum slope of the presynaptic AP. Right, 2-ms voltage steps were applied at 100 Hz. (B) Example traces of Ca^{2+} currents and capacitance increases (ΔCm) for different pulse durations at a dissociated cMF terminal (left). Average capacitance increases were plotted against pulse durations ($n = 10$; right). The data were fitted by a

single exponential with a time constant of 10.2 ms and a line with a slope of 49.8 fF s⁻¹. (C) Sizes of the bright spots for “diffuse”, “vanish”, “tethering”, and “tethering-vanish” events. Top, representative and average images for “diffuse”, “vanish”, “tethering”, and “tethering-vanish” events. Bottom, average standard deviation (sigma) of the fitted Gaussian (n = 8, 34, 32, and 34 for “diffuse”, “vanish”, “tethering”, and “tethering-vanish” events, respectively). Error bars show SEM. (D) Time course of the fluorescent intensity for “diffuse” events. A subset of vanish events showed the spreading of FM dye into the surrounding area. Top, average images of 8 spots. Middle, the fluorescence time course within a center (347 nm diameter) and a concentric annulus (347 nm inner and 867 nm outer diameters). Bottom, expanded fluorescence time course for the annulus. (E) Vesicle events recorded at high temperature from 26 terminals (30-31°C, using the depolarizing pulse to 0 mV for 100 ms). Peri-stimulus time histograms in the “vanish” and “tethering” types of events (top) and cumulative number of the events (bottom). The time period of the pulse is indicated by the grey color. The cumulative number of “vanish” and “tethering” events were fitted with a double exponential function and an exponential function, respectively. According to the result of the different pulse duration experiments (Fig. S1B), τ_1 for “vanish” events was fixed to 10 ms. The fit has a ratio of the amount of the 1st to 2nd component of 0.02.

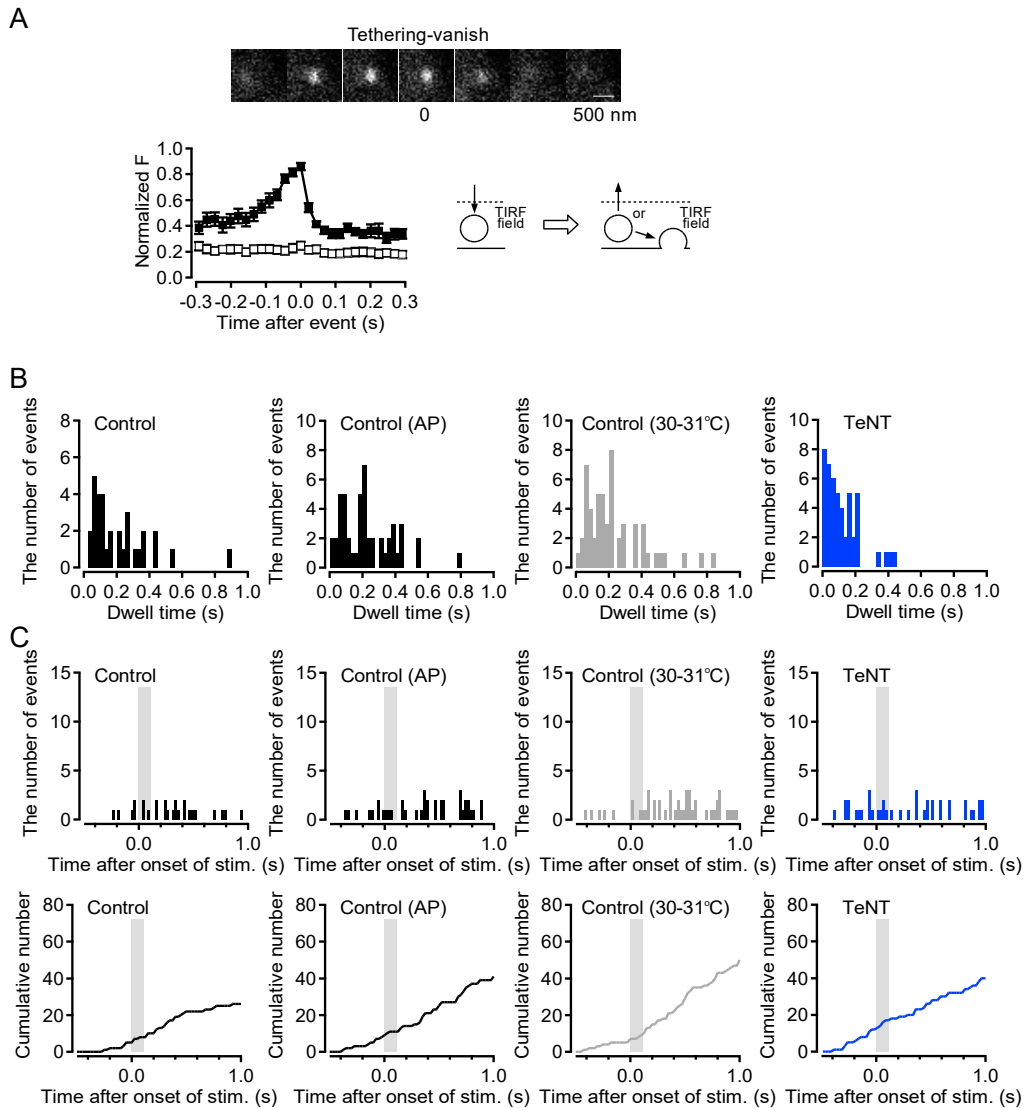


Fig. S2. “Tethering-vanish” events at dissociated cMF terminals in various experimental conditions. (A) Top, an example of the “tethering-vanish” events in TIRF image was shown. Bottom, averages of the normalized fluorescent intensity were plotted against time for a 347-nm diameter circle centered on the spot (filled squares) and the concentric annulus around the circle (outer diameter of 867 nm; open squares; $n = 26$). Error bars show SEM. “tethering-vanish” events correspond to vesicles that recruit to TIRF field, followed by moving out from the TIRF field or undergoing exocytosis during recording. (B) Histograms of dwell time of “tethering-vanish” events for control, AP, high temperature (30-31°C), and TeNT experiments (same panel as that in Fig. 2) from 56, 43, 26, and 26 terminals, respectively. (C) Peri-stimulus time histograms of “tethering-vanish” events and of cumulative numbers of these events. The time period of the pulse is indicated by the grey color.

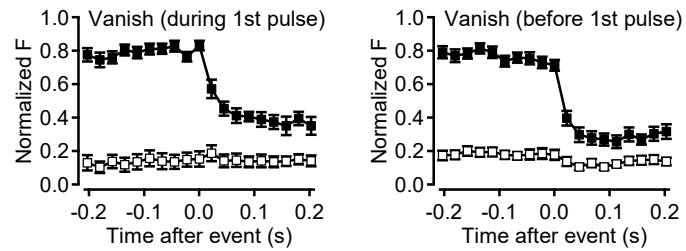


Fig. S3. Time course of the fluorescent intensity for “vanish” events in the double pulse experiments. Time courses of the fluorescence intensities within a center (347 nm diameter, filled squares) and a concentric annulus (347 nm inner and 867 nm outer diameters, open squares) for the vanish events during and before the 1st pulse in double pulse experiments from 48 terminals. Mean and SEM are shown. Half (50%) of vanish events during 1st pulse (0-30 ms, see Fig. 3) showed the spreading of FM dye into the surrounding area (n = 14, left). In contrast, a majority (97%) of the vanish events before 1st pulse (-0 ms) showed decrease of the fluorescent intensity in the surrounding area (n = 20, right).

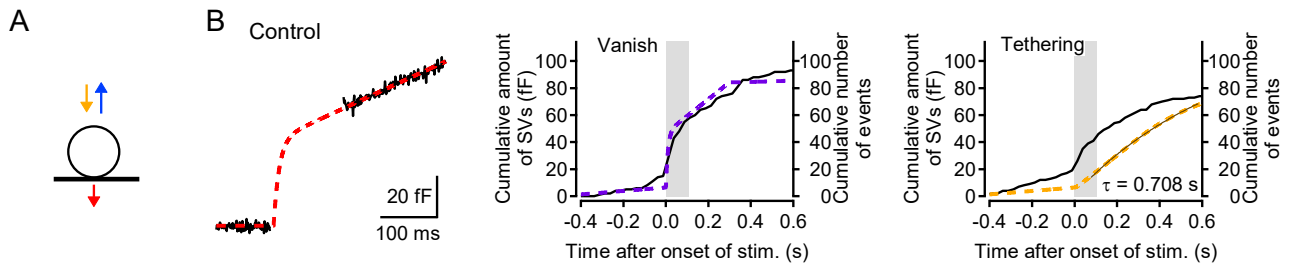


Fig. S4. Model simulation with an immediate priming after tethering.

(A) One pool model. We assumed a single RRP that could be released with a time constant of 10 ms (Fig. S1) and a vesicle tethering process. The model assumes that vesicle priming is immediate. (B) Fits of release and vanish events gave the rate constant of 12 s^{-1} for vesicle recruitment per a functional release site (see Methods). Dashed curves show the results of the model simulation. The dashed curve in red represents the fit of the vesicle release. The dashed curve in purple shows the vesicle movement indicated by blue and red arrows in A. Yellow curve shows vesicle recruitment to RRP. The yellow curve was fitted with a single exponential curve having a time constant of 708 ms that is slower than that in data.